

2010

# Analysis of Oil Film Force in Single Screw Compressor

Shuo Sun

*Xi'an Jiaotong University*

Weifeng Wu

*Xi'an Jiaotong University*

Xiaoling YU

*Xi'an Jiaotong University*

Quanke Feng

*Xi'an Jiaotong University*

Follow this and additional works at: <https://docs.lib.purdue.edu/icec>

---

Sun, Shuo; Wu, Weifeng; YU, Xiaoling; and Feng, Quanke, "Analysis of Oil Film Force in Single Screw Compressor" (2010).  
*International Compressor Engineering Conference*. Paper 2024.  
<https://docs.lib.purdue.edu/icec/2024>

This document has been made available through Purdue e-Pubs, a service of the Purdue University Libraries. Please contact [epubs@purdue.edu](mailto:epubs@purdue.edu) for additional information.

Complete proceedings may be acquired in print and on CD-ROM directly from the Ray W. Herrick Laboratories at <https://engineering.purdue.edu/Herrick/Events/orderlit.html>

## Analysis of Oil Film Force in Single Screw Compressor

Shuo Sun\*, Weifeng Wu, Xiaoling YU , Quanke Feng

School of Energy and Power Engineering, Xi'an Jiaotong University,  
Xi'an, 710049, China (86-29-82675258, soonure@gmail.com)

### ABSTRACT

Good oil lubrication is helpful to reduce star-wheel wear in single screw compressors with the result of increasing service life. To study the effects of oil lubrication, a simplified analytic model of oil film force is developed in this paper. Analysis results show that the torques caused by oil film in front-side and back-side of tooth are unbalanced and the composite torque has the same direction with star-wheel rotation. The above torque will result in unequal clearances in front-side and back-side of tooth and the side with smaller clearance is apt to generate wear. It is also found that machines with small displacement have better torque balance than those with large displacement so it can be deduced that the former has less serious wear than the latter, which is in accordance with the actual wear phenomenon.

### 1. INTRODUCTION

Wear on star-wheel, is one of the most important problems that need to be solved for single screw compressors. Due to wear, volumetric efficiency of compressors begins to drop after working for thousands of hours so single screw compressors can not show the good performance in theory during production practice. To solve this problem, much attention has firstly been paid on the tooth profiles because profile determines the motion characteristic of meshing pairs. Zimmern (1976) who is the first to develop single screw compressors proposes a column envelope profile based on the original straight line envelop profile. Furthermore, a multicolumn envelope profile is developed by Wu and Feng (2009). These improvements in tooth profiles distribute the contact area into a more extensive region with the result of reducing wear. But until now few actual applications are reported because manufacture problems are not well solved. In another hand, machining precision is also studied. It has great impact on service life in the initial stage of development. Zimmern (1992) puts forward a kind of machine tool using shape lathe tool to process the screw groove. However, with the development of special machine, the increment of machining precision has little contribution to the service life when precision has reach a certain level. Otherwise, the study of high anti-abrasion materials is also a way to raise the service life. The application of material of PEEK increases the service life by a large margin. But anti-abrasion of materials still can not satisfy the demand of service life. In the meanwhile, material costs need to be considered. Since the above studies have not solved the wear problem effectively, fluid lubrication which is directly related to abrasion problem should be taken into account. Post and Zwaans (1986a) carries out simulation computations on the oil flow in the clearance of tooth flank based on a finite-wide thrust bearing model including inertia effects. According to their analyses oil film force changes with the variation of clearance sizes and geometrical shapes and the star-wheel under the action of torques can reach a equilibrium position with no contact with screw under each rotating angle. But this conclusion can not be used to explain the wear phenomenon in practice.

In this paper, a simplified model in the ideal state that the clearances in front-side and back-side of star-wheel tooth are equal is developed to study the effects of oil film force. Although the ideal state may be different from the actual situation, it should be the best state to prevent wear. If the composite torque on star-wheel is completely in balance under the ideal state, the wear will be restricted to minimum. However the composite torque changes with the rotating angle and can not reach balance in every rotating angle. Therefore, unbalanced torque in the ideal state

under each rotating angle can be analyzed by the model proposed in this paper and the results can be used to direct further optimization.

## 2. GEOMETRIC MODEL

In order to calculate the oil film force on star wheel, compression chamber volume under different rotating angles needs to be obtained firstly and the pressure in the corresponding situation can be calculated. According to the motion feature of star wheel, calculations of compression chamber volume are discussed under two conditions:

Condition I is the rotating angle in the interval of Expression (1)

$$\phi_{swin} \leq \phi_{sw} < \phi_{swmid} \tag{1}$$

Condition II is the rotating angle in the interval of Expression (2)

$$\phi_{swmid} \leq \phi_{sw} \leq \phi_{swout} \tag{2}$$

where

$\phi_{swin}$  is the rotating angle under which closing volume in the screw groove just forms.

$\phi_{swmid}$  is the rotating angle under which the top end of star-wheel tooth begins to break away from the screw groove,

$\phi_{swout}$  is the rotating angle under which the whole tooth just breaks away from the screw groove,

Compression chamber volume is calculated by double integration. Firstly the area element on star-wheel tooth surface is selected as shown in Figure 1. Secondly the volume element is obtained by using the above area element to sweep the screw groove. Finally double integration is computed to get the volume.

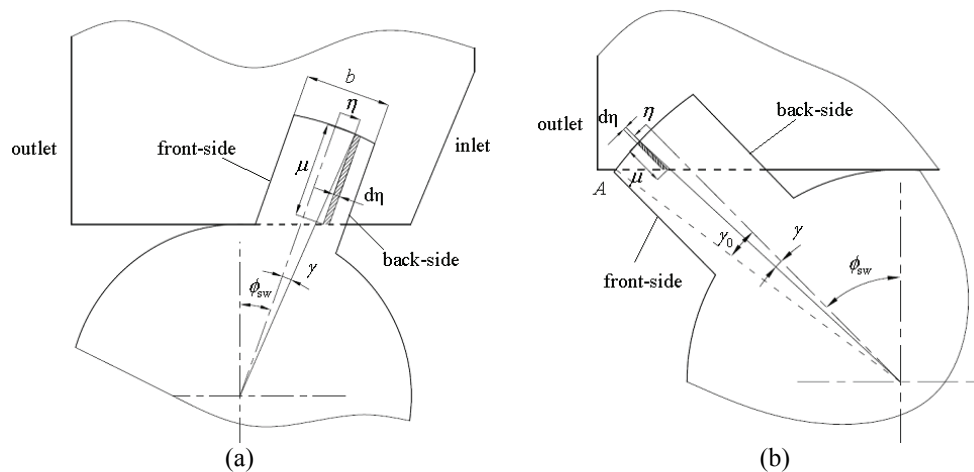


Figure 1 : Computation of compression chamber volume: (a) Condition I (b) Condition II

Area element  $dS$  shown by shadow region of Figure 1 is expressed by Equation (3)

$$dS = \mu d\eta \tag{3}$$

where  $\mu$  is derived by  $\eta$  in Equation (4).

$$\mu = \sqrt{R_{sw}^2 - \eta^2} - \eta \tan \phi_{sw} - \frac{a - R_{sr}}{\cos \phi_{sw}} \tag{4}$$

where  $R_{sr}$  is the radius of screw,  $R_{sw}$  is the radius of star-wheel and  $a$  is the center distance.

For Condition I shown in Figure 1(a), compression chamber volume is calculated by double integration with respect to  $\phi_{sw}$  and  $\eta$  in Equation(5)

$$V_1 = \frac{P}{2} \int_{\phi_{swin}}^{\phi_{swmid}} \int_{\frac{b}{2}}^{\frac{b}{2}} \frac{R_{sr}^2 - \left( a - \sqrt{R_{sw}^2 - \eta^2} \cos \phi_{sw} + \eta \sin \phi_{sw} \right)^2}{\cos \phi_{sw}} d\eta d\phi_{sw} \tag{5}$$

For Condition II shown in Figure 1(b), compression chamber volume is calculated in the similar method as Condition I but in the different integral interval.

Assume  $\gamma_0$  shown in Figure 1(b) as the included angle between the radius in Point A (the crossing point of the star-wheel tooth tip and screw outer edge) and the center line of star-wheel tooth, which is expressed in Equation (6)

$$\gamma_0 = \arccos\left(\frac{a - R_{sr}}{R_{sw}}\right) - \phi_{sw} \tag{6}$$

Compression chamber volume is calculated by double integration with respect to  $\phi_{sw}$  and  $\eta$  in Equation (7)

$$V_2 = \frac{P}{2} \int_{\phi_{swmid}}^{\phi_{swout}} \int_{-\frac{b}{2}}^{R_{sw} \sin \gamma_0} \frac{R_{sr}^2 - \left(a - \sqrt{R_{sw}^2 - \eta^2} \cos \phi_{sw} + \eta \sin \phi_{sw}\right)^2}{\cos \phi_{sw}} d\eta d\phi_{sw} \tag{7}$$

According to Equation (5) and (7), basic volume is derived by

$$V_0 = V_1 + V_2 \tag{8}$$

Therefore compression chamber volume under different rotating angles can be obtained by subtracting sweeping volume from basic volume.

$$V(\phi_{sw}) = \begin{cases} V_0 - \frac{P}{2} \int_{\phi_{swin}}^{\phi_{sw}} \int_{-\frac{b}{2}}^{\frac{b}{2}} f(\phi_{sw}, \eta) d\eta d\phi_{sw} & \phi_{swin} \leq \phi_{sw} < \phi_{swmid} \\ V_2 - \frac{P}{2} \int_{\phi_{swmid}}^{\phi_{sw}} \int_{-\frac{b}{2}}^{R_{sw} \sin \gamma_0} f(\phi_{sw}, \eta) d\eta d\phi_{sw} & \phi_{swmid} \leq \phi_{sw} \leq \phi_{swout} \end{cases} \tag{9}$$

where

$$f(\phi_{sw}, \eta) = \frac{R_{sr}^2 - \left(a - \sqrt{R_{sw}^2 - \eta^2} \cos \phi_{sw} + \eta \sin \phi_{sw}\right)^2}{\cos \phi_{sw}} \tag{10}$$

### 3. ANALYSIS OF OIL FILM FORCE

In this paper, oil flow in the clearance of tooth flank is assumed as a single-phase steady flow in order to simplify the calculation and boundary conditions of pressure in two ends of the computational domain are respectively compression chamber pressure and suction pressure. The pressure in compression chamber under different rotating angles can be expressed as

$$p(\phi_{sw}) = \begin{cases} p_0 & \phi_{sw} < \phi_{swin} \\ \frac{V_0^n}{V(\phi_{sw})^n} p_0 & \phi_{swin} \leq \phi_{sw} < \phi_{swd} \\ p_d & \phi_{sw} \geq \phi_{swd} \end{cases} \tag{11}$$

$\phi_{swd}$  is the rotating angle under which exhaust process begins

According to the analysis of Post and Zwaans (1986b) oil flow in single screw compressors is similar to the bearing lubrication but the Reynolds equation is not applicable to compressors because inertia force under high relative velocity can not be neglected. Therefore, computational methods in consideration of inertia effects are needed.

According N-S equation,

$$\frac{\partial U}{\partial t} + (U \cdot \nabla)U = -\frac{1}{\rho} \nabla p + \frac{1}{\rho} \nabla \cdot (2\mu S + \lambda \delta \nabla \cdot U) + f \tag{12}$$

The second term of the left-hand side of Equation (12) is inertia term. The equation with inertia term is non-linear which is difficult to be solved directly. In order to simplify the simulation calculation Post and Zwaans (1986c) adopted the method proposed by Launder and Leschziner (1978a) which turns N-S equation into a linear one by the introduction of the mean velocity  $u_m$ . In this paper, the simplified model on neglecting gradients of tooth length direction in the paper of Launder and Leschziner (1978b) is adopted which is shown in Equation (13). Because the tooth length is usually more than five times of the tooth thickness, this simplification is acceptable in engineering calculation.

$$\frac{dp}{dx} = \frac{12\mu}{h^2} \left( \frac{U}{2} - u_m \right) + \frac{\rho}{h} (\alpha u_m^2 - \gamma U^2) \frac{dh}{dx} \quad (13)$$

where

$$\alpha = 1.2, \gamma = 0.133$$

and  $h(x)$  is the width of oil flow channel in different location.

According to continuity equation

$$\frac{d}{dx}(\rho h u_m) = 0 \quad (14)$$

the term of  $\rho h u_m$  does not vary with  $x$  so it can be set to a constant  $M$

And Equation (13) can be simplified for

$$\frac{dp}{dx} = \frac{6\mu U}{h^2} - \frac{12\mu M}{\rho h^3} + \alpha \frac{M^2}{\rho h^3} \frac{dh}{dx} - \frac{\rho}{h} \gamma U^2 \frac{dh}{dx} \quad (15)$$

where

$$M = \rho h u_m$$

Integral with respect to  $x$  in both sides of Equation(15) is expressed as

$$\int_{x_0}^x \frac{dp}{dx} dx = \int_{x_0}^x \frac{6\mu U}{h^2} dx - \frac{12\mu M}{\rho} \int_{x_0}^x \frac{1}{h^3} dx + \alpha \frac{M^2}{\rho} \int_{x_0}^x \frac{1}{h^3} \frac{dh}{dx} dx + \int_{x_0}^x \left( -\frac{\rho}{h} \gamma U^2 \frac{dh}{dx} \right) dx \quad (16)$$

Boundary conditions are obtained from the pressure solved in Equation (11)

$$p(x_0) = p_0, \quad p(x_1) = p(\phi_{sw}) \quad (17)$$

Equation (17) is introduced into Equation (16) to get the pressure distribution as

$$p(x) = p_0 + \int_{x_0}^x \frac{6\mu U}{h^2} dx - \frac{12\mu M}{\rho} \int_{x_0}^x \frac{1}{h^3} dx - \alpha \frac{M^2}{2\rho} \left( \frac{1}{h(x)^2} - \frac{1}{h(x_0)^2} \right) - \rho \gamma U^2 [\ln h(x) - \ln h(x_0)] \quad (18)$$

where

$$M = \frac{\frac{12\mu}{\rho} \int_{x_0}^{x_1} \frac{1}{h^3} dx - \sqrt{\left( \frac{12\mu}{\rho} \int_{x_0}^{x_1} \frac{1}{h^3} dx \right)^2 + \frac{2\alpha}{\rho} \left( \frac{1}{h(x_1)^2} - \frac{1}{h(x_0)^2} \right) T}}{-\alpha \left( \frac{1}{h(x_1)^2} - \frac{1}{h(x_0)^2} \right)}$$

$$T = -p(\phi_{sw}) + p_0 + \int_{x_0}^{x_1} \frac{6\mu U}{h^2} dx - \rho \gamma U^2 [\ln h(x_1) - \ln h(x_0)]$$

Area element  $dS$  on the location  $(u, t)$  of tooth flank is selected.  $l$  is the location in tooth length direction and  $t$  is the location in tooth thickness direction.

$$dS = dl dt \quad (19)$$

The torque element caused by oil film force is derived as

$$dT = [p(t) - p_0](l + K) dt du \quad (20)$$

and  $K$  is the radius at the root of tooth.

Maximum value of  $l$  in the above equation equals to  $H$  which is the length of tooth and minimum value of  $l$  can be solved by the following equation.

$$l_{\min} = \begin{cases} H - \mu(b/2) & \text{for front-side of tooth} \\ H - \mu(-b/2) & \text{for back-side of tooth} \end{cases} \quad (21)$$

The expression of  $\mu(\eta)$  is shown in Equation (4)

The torque is derived from integral as

$$T = \int_{l_{\min}}^H \int_{f_0}^{f_1} dT \quad (22)$$

The difference between the torque on the front-side and that on the back-side is as follows

$$T_n(\phi_{sw}) = T_{back} - T_{front} \quad (23)$$

For the eleven-tooth star-wheel, there are at most four teeth under engagement simultaneously so the total torque on the star-wheel can be expressed as

$$T(\phi_{sw}) = \sum_{k=n}^4 T_n \left[ \phi_{sw} + (n-1) \frac{2\pi}{11} \right] \quad (24)$$

#### 4. RESULTS

In this paper, single screw compressor with the straight line cross-section is chosen for the calculated example. Air displacements of 1.5m<sup>3</sup>/min and 6 m<sup>3</sup>/min are respectively calculated. Pressure distribution under the rotating angle of 0 deg in front-side of tooth for the displacement of 1.5m<sup>3</sup>/min are shown in Figure 2.  $\delta$  is the clearance in tooth flank. The pressure in the upstream region ( $x > 3$ ) of oil flow appears a wave crest which is located near the minimum width ( $x=3$ ) and the maximum value is increasing with the decrement of  $\delta$ . This pressure distribution is caused by combined action of inertia force and shearing force. The pressure in the downstream region ( $x < 3$ ) of oil flow appears negative value. According to bearing lubrication theory, air pockets may appear in negative pressure region during real process, so the pressure in the negative pressure region is simplified as suction pressure in this paper. Therefore the oil film torques on star-wheel under different rotating angles can be calculated based on the modified pressure distribution. The results are shown in Figure 3(a).

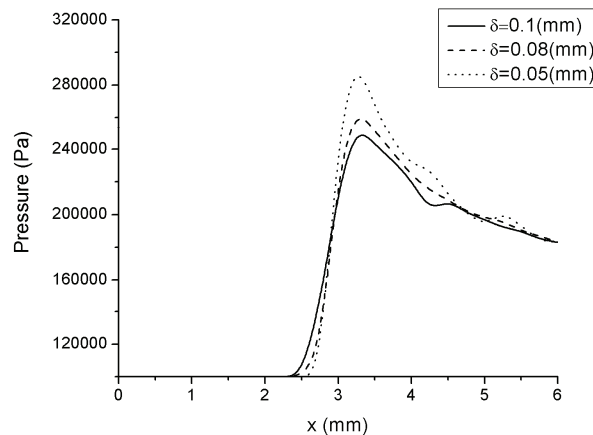


Figure 2 Pressure distribution of oil film in front-side of tooth

The oil film torque changes with the rotating angle and the values of torque under different rotating angles are all positive. According to Equation (23), the results show that star-wheel is under the action of a torque whose direction is same with the rotation direction of star-wheel. According to the test by Zhou and Jin (1998), the mean bearing resistance torque for machines with air displacement of 1.5m<sup>3</sup>/min is 0.3Nm. The composite torque caused by oil film forces and bearing resistances for machines with air displacement of 1.5m<sup>3</sup>/min is shown in Figure 3(b). This

torque appears a periodic change. This composite torque will cause unequal clearances in front-side and back-side of tooth which will make star-wheel prone to contact with screw grooves. For machines with small displacement like the displacement of  $1.5\text{m}^3/\text{min}$ , the torque appears symmetrical in positive and negative directions and the maximum torque is only  $0.212\text{Nm}$ . Hence it can explain the phenomenon that in productive practice machines with small displacement have relatively good performance and the wear problem is not serious. However for machines with large displacement like the displacement of  $6\text{m}^3/\text{min}$ , the mean torque caused by oil film force is almost eight times of that in the small machines and the resistance torque has usually not such a large increment as oil film torque. Therefore, the composite torque on the star-wheel can reach a much larger positive value than that of small machines. It may cause more serious wear especially in front-side of tooth, which is in accordance with the actual wear phenomenon.

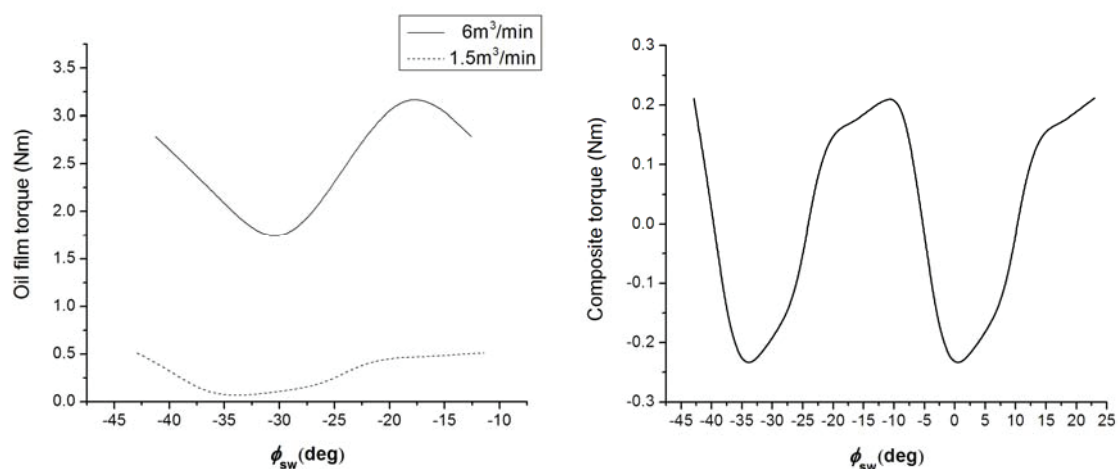


Figure 3 Oil film torque on star-wheel (a) Oil film torque (b) Composite torque

## 5. CONCLUSION

In this paper, analysis of oil film force on star-wheel is carried out. A simplified model with equal clearances in front-side and back-side of tooth is presented. The following conclusions can be drawn by the calculation results:

1. The torques caused by oil film force in front-side and back-side of tooth are not in balance. The composite torque of front-side and back-side of tooth has the same direction with the star-wheel rotation which may change the clearances of tooth flank with the result of increasing the probability of wear.
2. The composite torques caused by oil film force are different for machines with different displacements. The machines with large displacement have bigger composite torque than machines with small displacement.
3. The torque caused by oil film force mainly depends on the area size which is under the action of high pressure in the same working situation.

In order to reduce wear of tooth flank, the composite torque caused by oil film force should be reduced according to the analysis in this paper. Therefore the further studies have to be carried out in the optimization of the shape parameters of tooth flank. The computing model proposed in this paper can be used to direct the optimization.

## REFERENCES

- Zimmern B., 1992, Process to Cut Hour Glass Screws, US Pat, USA, 5,084,965.
- Zimmern B., 1976, Rotary Inter-engaging Worm and Worm Wheel with Specific Tooth Shape, US Pat, USA, 3,932,077.
- Zhou L., Jin GX., 1998, Dynamic Characteristics of Gate Rotor for Single Screw Compressor, J Xi'an Jiaotong Univ, vol. 32, No. 11 : p. 58-62
- WU WF., FENG QK., 2009, A Multicolumn Envelope Meshing Pair for Single Screw Compressors, *ASME J Mech. Des.*, vol. 131, no.7 : p.074505
- Post W., Zwaans M., 1986, Computer Simulation of the Hydrodynamic Lubrication in A Single Screw Compressor, *Compressor Technology Conference, Purdue* : p. 334-348.
- Lauder, B.E., Leschziner, M., 1978, Flow in Finite-Width, Thrust Bearings Including Inertial Effects, *J LUBRIC TECH-T ASME*, vol. 100 : p. 330-338

### ACKNOWLEDGEMENT

We are grateful to Jian Li for his valuable discussions and helpful advices